

Supporting Information

Turning Water from a Hindrance to the Promotor of Preferential Electrochemical Nitrogen Reduction

Charlynn Sher Lin Koh,^a Hiang Kwee Lee,^{a, b} Howard Yi Fan Sim,^a Xuemei Han,^a Gia Chuong Phan-Quang^a and Xing Yi Ling*

^aDivision of Chemistry and Biological Chemistry, School of Physical and Mathematical Sciences, Nanyang Technological University, Singapore 637371.

^bDepartment of Materials Science and Engineering, Stanford University, Stanford, CA 94305, USA .

*Email: xyling@ntu.edu.sg

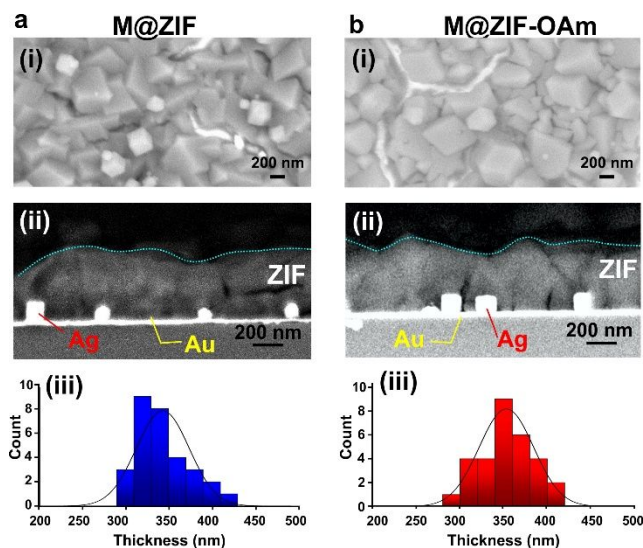


Figure S1. Characterization of M@ZIF before and after oleylamine functionalization. (a) Before functionalization and (b) after functionalization with oleylamine. (i) Top view SEM image of ZIF. (ii) Cross-sectional SEM images of the M@ZIF platforms. (iii) ZIF thickness distribution.

Top view and cross-sectional SEM images after functionalization with oleylamine reveals minimal change in the thickness and structure of the ZIF overgrowth. The cracks appearing in both the ZIF-only and ZIF-OAm substrates are due to the electron-induced damage of the ZIF surface at high voltage during imaging. Hence, the functionalization process increases the hydrophobicity of the ZIF surface while still maintaining the full encapsulation of the electrode.

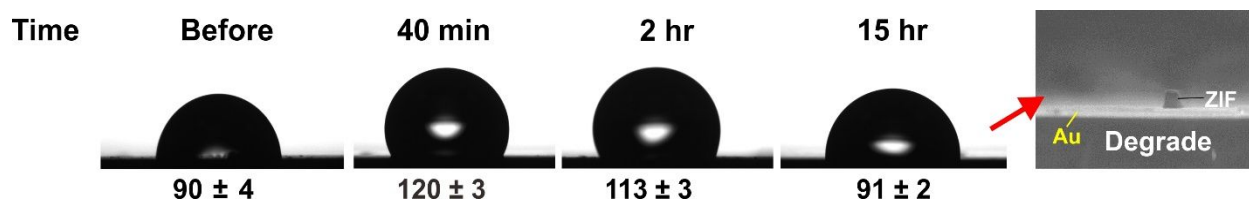


Figure S2. Contact angle measurements of ZIF film substrates after functionalization with 0.1 M oleylamine at different reaction parameters.

In order to functionalize ZIF surface with oleylamine, the ZIF films were immersed in oleylamine solutions for different times and under different temperature. Upon immersion and incubation for 40 min, the contact angle measured increased from $(90 \pm 4)^\circ$ to $(120 \pm 3)^\circ$, indicating the successful functionalization of oleylamine. At much longer immersion periods, the ZIF film degrades due to the excessive functionalization on the ZIF surface. This film degradation thus results in a drop in the contact angle after immersion overnight. Hence, the optimized incubation time for functionalization is set at 40 min under ambient conditions.

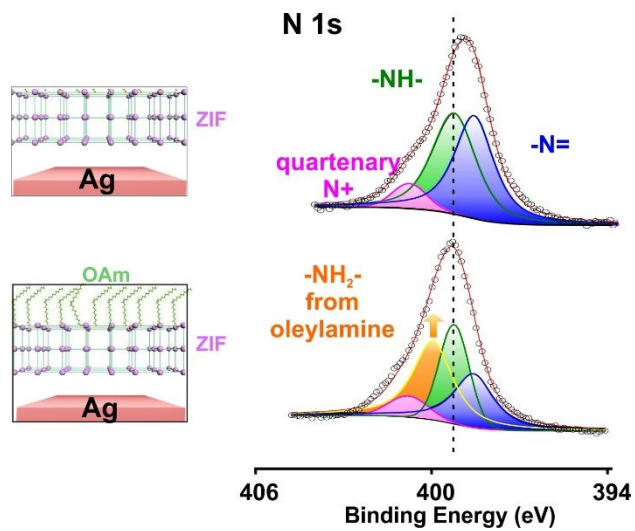


Figure S3. High resolution XPS scans of N 1s region of ZIF without (top) and with (bottom) oleylamine functionalization.

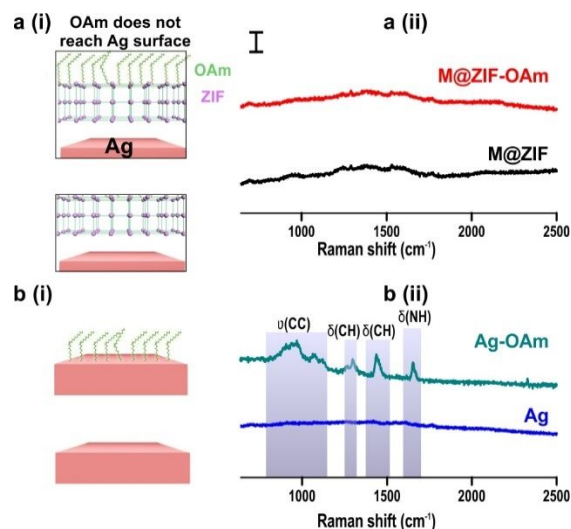


Figure S4. SERS spectra of M@ZIF before and after oleylamine functionalization. (a) Scheme (i) and SERS spectra (ii) when Ag@ZIF is functionalized with ZIF and (b) Ag-only platform functionalized with OAm. No oleylamine vibrational peaks are observed when Ag is encapsulated by ZIF. This is in contrast with the oleylamine peaks present after bare HCl-treated Ag is immersed under the same functionalization conditions.

We affirm that the functionalization of oleylamine occurs only at the surface of ZIF by measuring the SERS signal before and after oleylamine functionalization. In the absence of ZIF, where only HCl treated Ag nanocubes are used, the functionalization of oleylamine results in the emergence of peaks that are due to the C-C stretching, C-H and NH₂ bending of oleylamine. However, for Ag@ZIF films, the SERS spectra remains relatively unchanged, indicating that the oleylamine is unable to penetrate through ZIF to reach the SERS-active Ag nanocubes surface.

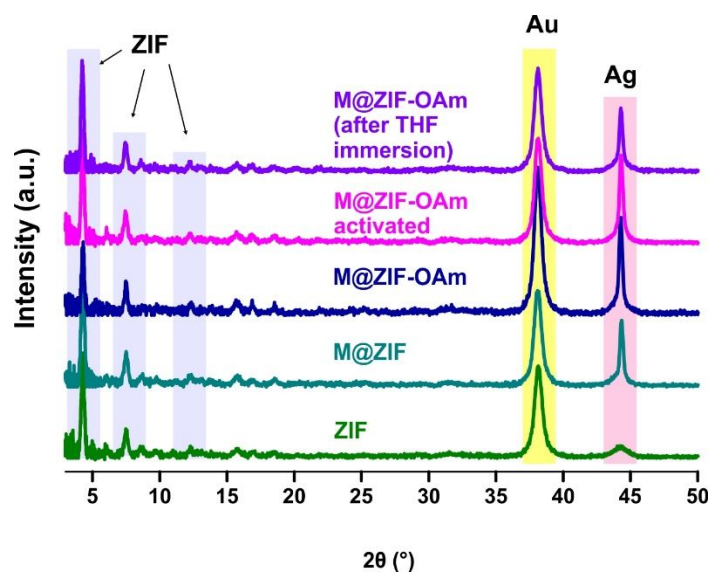


Figure S5. Substrate XRD diffraction pattern of as-synthesized ZIF, M@ZIF, M@ZIF-OAm, thermal-activated M@ZIF-OAm and M@ZIF-OAm immersed in the THF-based electrolyte for approximately 6 h (from bottom to top).

Supporting Information 1 – calculation of moisture content in air

The calculation of the moisture content in air is calculated below:

According to Guide to Meteorological Instruments and Methods of Observation, World Meteorological Organization, 2008, the saturation vapor pressure (e_w) at 298 K, 1 atm is 31.75 hPa. Given that the average relative humidity (RH) in Singapore is 80%, the actual vapor pressure (e) is given by:

$$e = e_w \frac{RH}{100} = 31.75 \times 0.80 = 25.4 \text{ hPa}$$

Using the ideal gas law,

$$pV = nRT$$
$$eV = \frac{m}{M}RT$$

Where p is the partial pressure ($= e$) at ambient temperature ($T = 298 \text{ K}$), m is the mass of water, M is its molecular weight and R is the universal gas constant, 8.31 J/K.mol .

The mass of water vapor per unit volume of air can thus be obtained by rearranging the equation:

$$\frac{m}{V} = \frac{eM}{RT} = \frac{2450 \times 18.0152}{8.31 \times 298} = 18 \text{ g/m}^3$$

Given that the nitrogen gas flow is 3 sccm for a total of 360 min, the total volume of gas is 1080 cm^3 . By determining the overall volume of gas used, this translates to the total mass of water accumulated if ambient air is used:

$$\text{Mass} = \frac{3 \times 360}{10^6} \times 18 = 0.0194 \text{ g}$$

$$\%v/v = \frac{0.0194}{9} \times 100 = 0.216 \%$$

Hence, when using ambient air as the N₂ source, the amount of water accumulating in the electrolyte reaches 0.216%. This estimated water content is crucial as a reference that should be taken in consideration when designing NRR systems that are geared toward realizing ambient air-to-ammonia conversion.

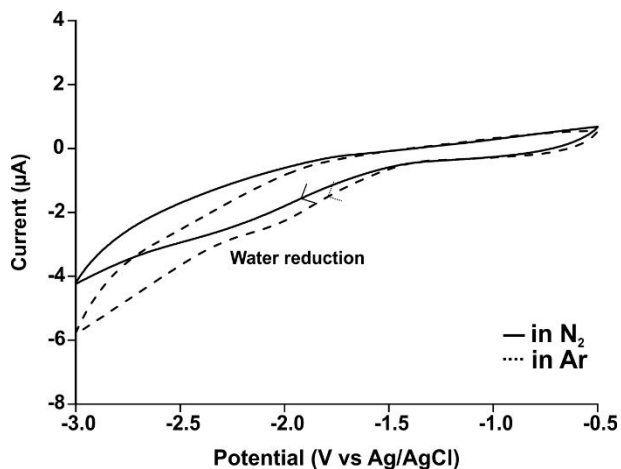


Figure S6. CV response of M@ZIF-oleylamine electrode in electrolyte containing ethanol instead of butanol as molecular filler. The same molecular size of ethanol makes it to be a less efficient molecular filler compared to butanol which results in HER evolution. The electrochemical investigation is performed in a three-electrode electrochemical setup. Pt wire and Ag/AgCl (1 M KCl) are used as counter (CE) and reference electrodes (RE), respectively.

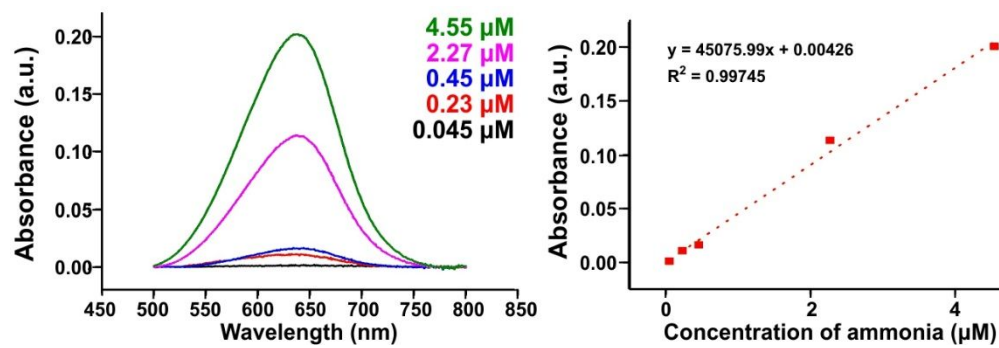


Figure S7. Absorption spectra of indophenol blue at various concentration and the linear correlation of the absorbance intensity to the effective concentration of ammonium ions present to enable indophenol blue formation.

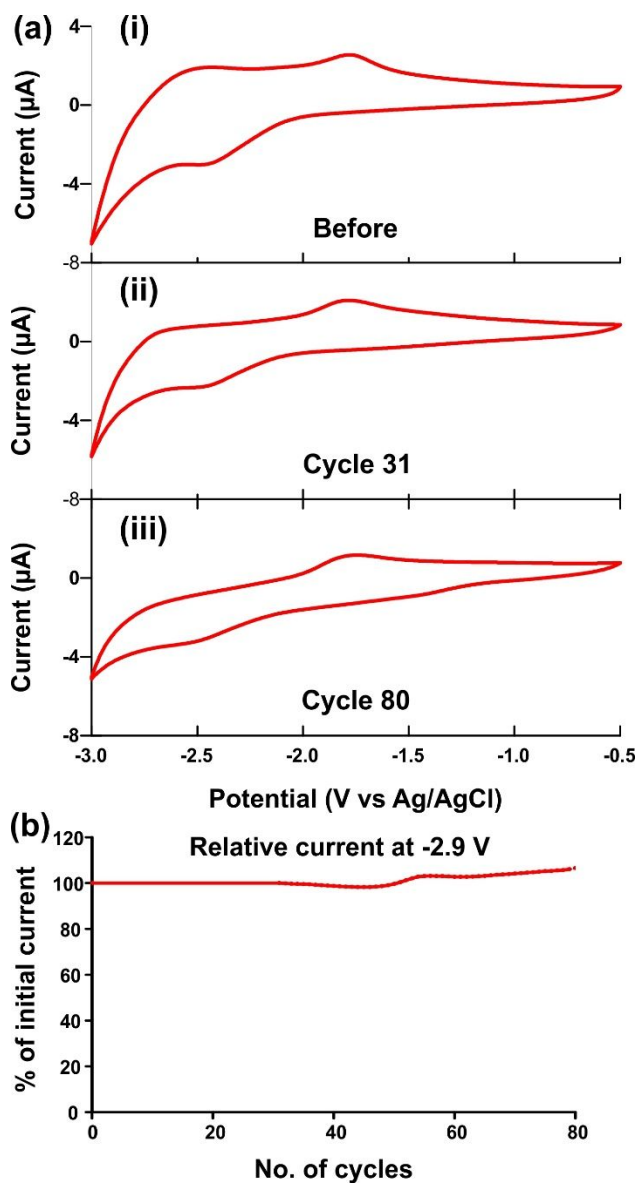


Figure S8. (a)(i-iii) Continuous cyclic voltammograms depicting electrochemical responses under N_2 using M@ZIF-OAm electrode for 80 cycles. (b) Percentage of current density relative to initial current at -2.9 V as the M@ZIF-OAm is subjected to continuous cyclic voltammetry for 80 cycles. The consistent and sustained current density across the number of cycles demonstrate the high stability of our catalytic system.

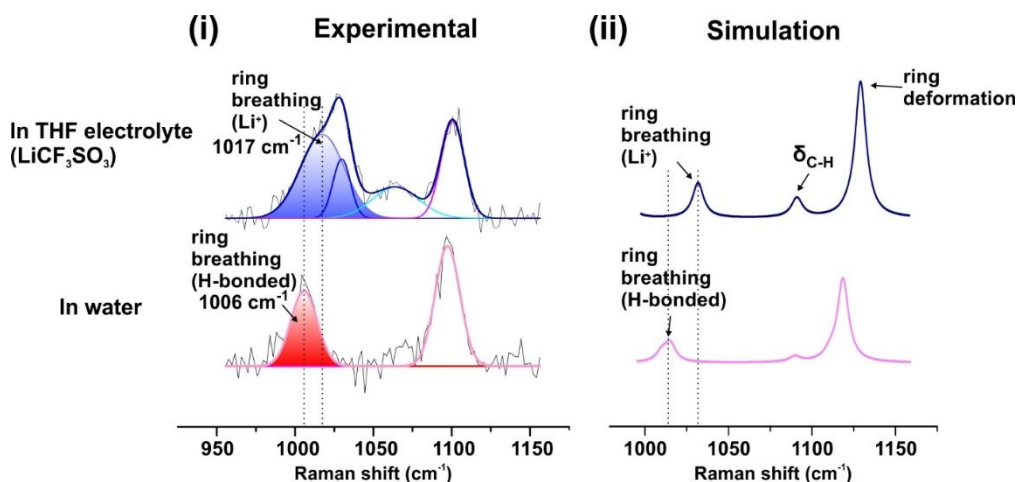


Figure S9. Experimental and simulated SERS spectra of mercaptopyridine when immersed in THF electrolyte containing Li salt and in water, respectively.

When immersed in THF electrolyte, the MPy SERS spectra shows a dominant peak at 1017 cm^{-1} which can be ascribed to its ring breathing mode. When immersed in water, this ring breathing mode is red shifted to 1006 cm^{-1} . By employing density functional theory (DFT) simulation, we reveal that the peak at 1017 cm^{-1} emerges when MPy is immersed in THF. This is likely due to the presence of Li salt in the electrolyte (0.1 M), where the positively charged Li^+ stabilizes the aromatic ring. Similarly in the case of water, N-atom in MPy experiences hydrogen bonding with water hence result in the stabilization of aromatic ring. However, the extent of stabilization is lower in the presence of water compared to Li^+ which causes the ring breathing mode to red shift when MPy is immersed in water instead. On the other hand, the addition sharp peak at 1028 cm^{-1} can be ascribed to the MPy breathing mode when the N-atom is binded in a network, such as ZIF, when the N-atom interacts with the Zn atoms from the ZIF network.

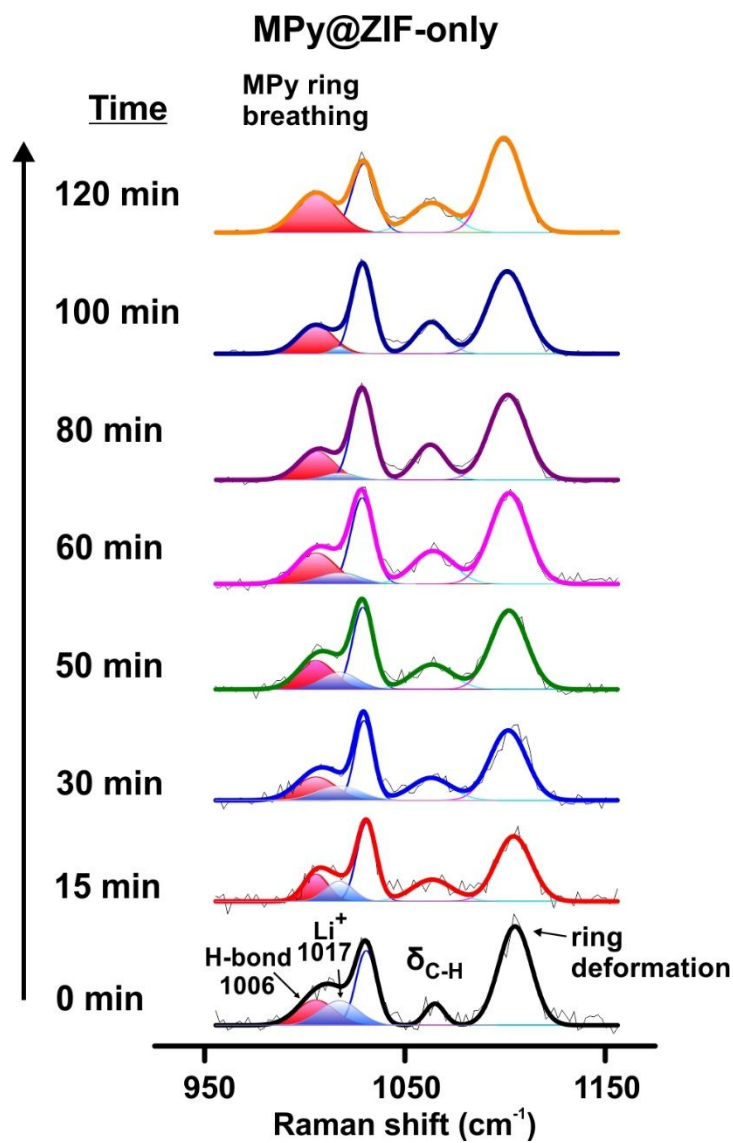


Figure S10. Time-resolved SERS spectra of Ag-MPy-Au@ZIF sample immersed in THF electrolyte after the addition of water. Shaded regions depict the deconvoluted peaks at the breathing mode of the MPy probe. The peak at 1006 cm^{-1} is indexed to the hydrogen-bonded MPy breathing mode (red) that arises due to the diffusion of water molecules to the Ag surface. The peak at 1017 cm^{-1} (blue) is ascribed to the MPy breathing mode when Li^+ ions from the electrolyte interacts with N-atom of MPy.

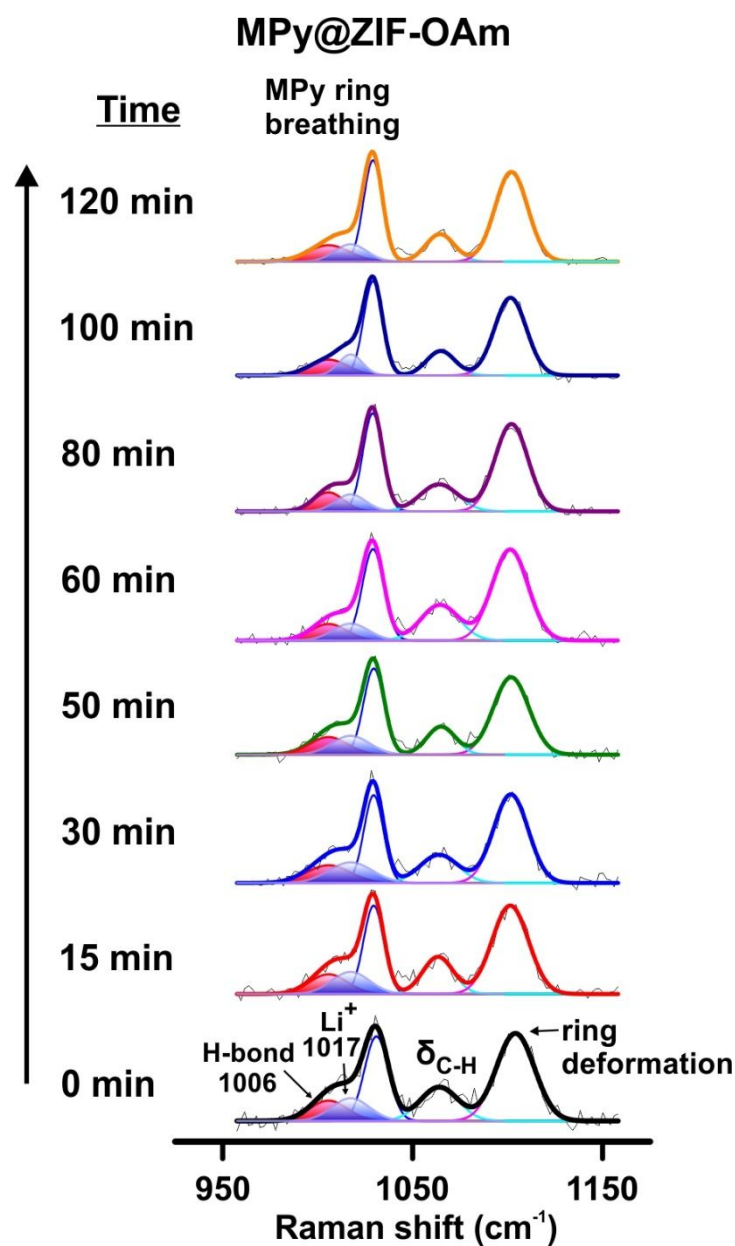


Figure S81. Time-resolved SERS spectra of the Ag-MPy-Au@ZIF-OAm sample immersed in THF electrolyte after the addition of water. Shaded regions depict the deconvoluted peaks at the breathing mode of the MPy probe. The peak at 1006 cm⁻¹ is indexed to the hydrogen-bonded MPy breathing mode (red) that arises due to the diffusion of water molecules to the Ag surface. The peak at 1017 cm⁻¹ (blue) is ascribed to the MPy breathing mode when Li⁺ ions from the electrolyte interacts with N-atom of MPy.

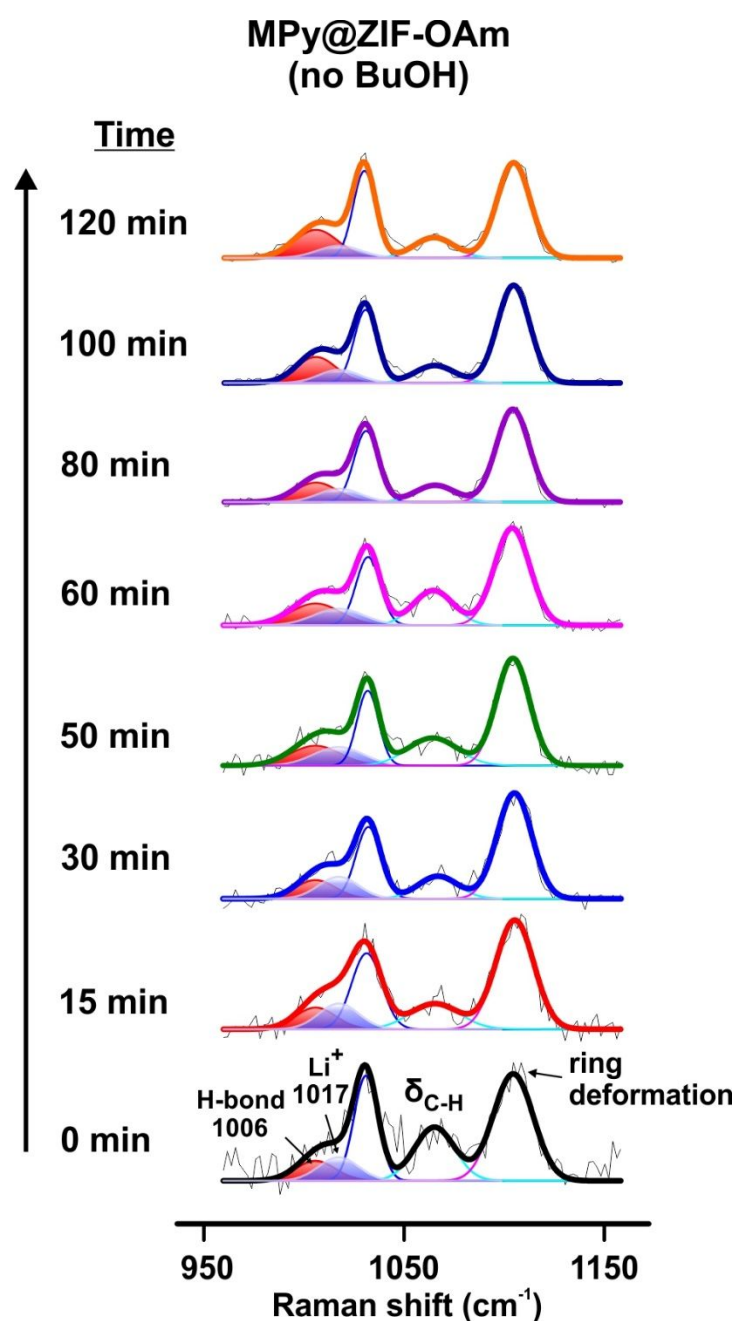


Figure S92. Time-resolved SERS spectra of the Ag-MPy-Au@ZIF-OAm sample immersed in THF electrolyte without BuOH as the filler after the addition of water. Shaded regions depict the deconvoluted peaks at the breathing mode of the MPy probe. The peak at 1006 cm⁻¹ is indexed to the hydrogen-bonded MPy breathing mode (red) that arises due to the diffusion of water molecules

to the Ag surface. The peak at 1017 cm^{-1} (blue) is ascribed to the MPy breathing mode when Li^+ ions from the electrolyte interacts with N-atom of MPy.

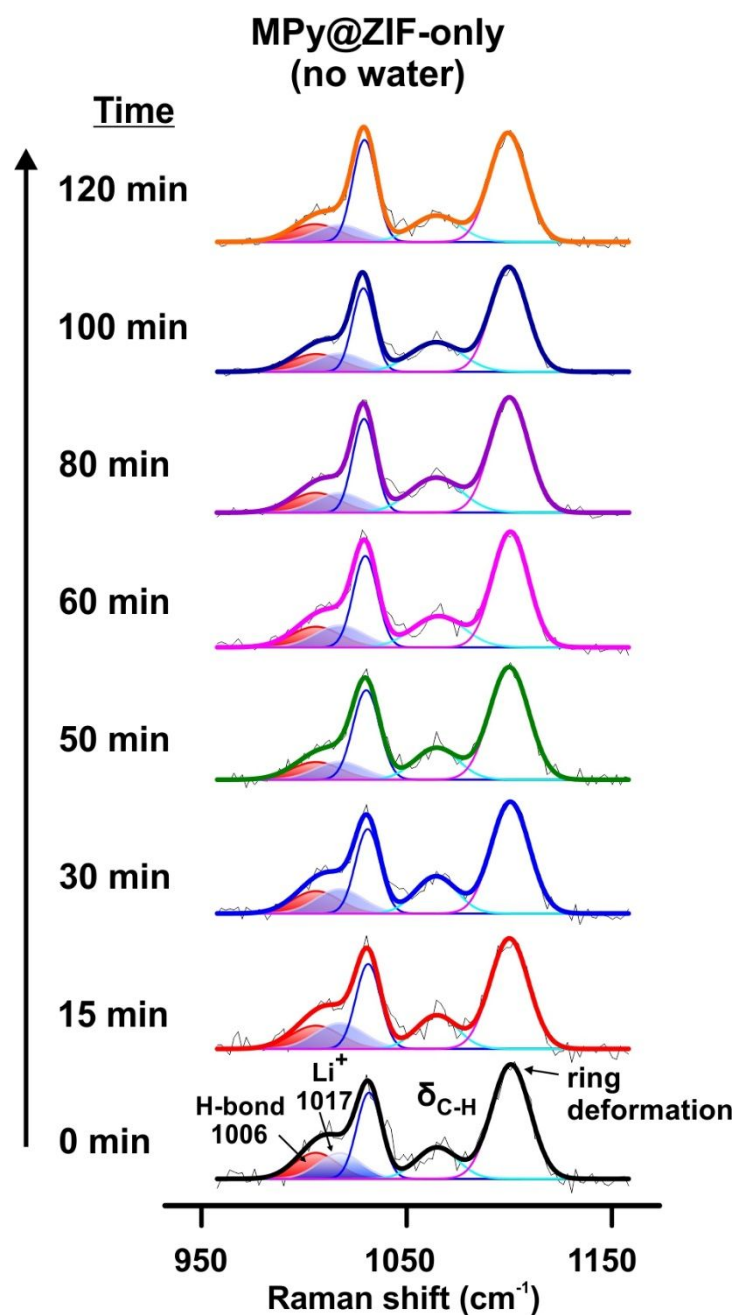


Figure S10. Control experiment involving the time-dependent SERS spectra of Ag-MPy-Au@ZIF substrate immersed in THF electrolyte without addition of water. Shaded regions depict the deconvoluted peaks at the breathing mode of the MPy probe. The peak at 1006 cm⁻¹ is indexed to the hydrogen-bonded MPy breathing mode (red) that arises due to the diffusion of water molecules

to the Ag surface. The peak at 1017 cm^{-1} (blue) is ascribed to the MPy breathing mode when Li^+ ions from the electrolyte interacts with N-atom of MPy.

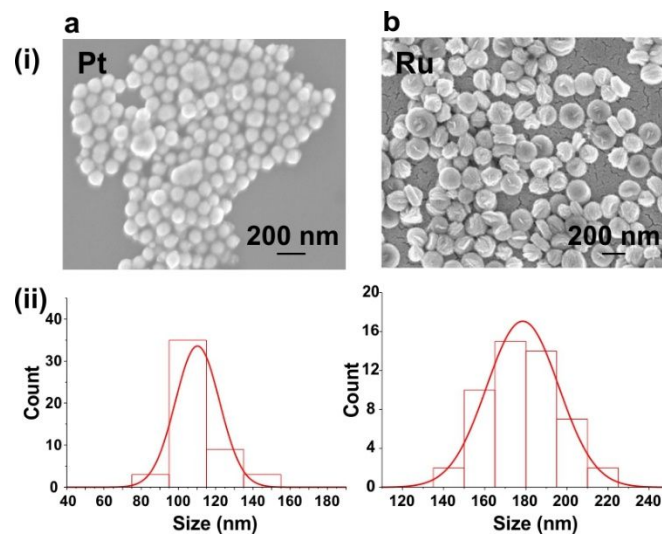


Figure S11. Characterization of metallic electrocatalysts. Characterization of a Platinum nanoparticles and b Ruthenium nanoparticles. (i) SEM images and (ii) Size distribution of respective nanoparticles.

References

1. Lee, H. K.; Lee, Y. H.; Phang, I. Y.; Wei, J.; Miao, Y.-E.; Liu, T.; Ling, X. Y., Plasmonic Liquid Marbles: A Miniature Substrate-less SERS Platform for Quantitative and Multiplex Ultratrace Molecular Detection. *Angew. Chem. Int. Ed.* **2014**, *53* (20), 5054-5058.
2. Tsuneto, A.; Kudo, A.; Sakata, T., Lithium-mediated electrochemical reduction of high pressure N₂ to NH₃. *J. Electroanal. Chem.* **1994**, *367* (1), 183-188.
3. Yun, D. S.; Joo, J. H.; Yu, J. H.; Yoon, H. C.; Kim, J.-N.; Yoo, C.-Y., Electrochemical ammonia synthesis from steam and nitrogen using proton conducting yttrium doped barium zirconate electrolyte with silver, platinum, and lanthanum strontium cobalt ferrite electrocatalyst. *J. Power Sources* **2015**, *284*, 245-251.